

Swell Transformation across the Continental Shelf. Part II: Validation of a Spectral Energy Balance Equation

FABRICE ARDHUIN

Centre Militaire d'Océanographie, Service Hydrographique et Océanographique de la Marine, Brest, France

T. H. C. HERBERS, P. F. JESSEN, AND W. C. O'REILLY

Department of Oceanography, Naval Postgraduate School, Monterey, California

(Manuscript received 23 July 2002, in final form 27 December 2002)

ABSTRACT

State-of-the-art parameterizations of the interactions of waves with a sandy bottom are evaluated using extensive field observations of swell evolution across the North Carolina continental shelf and hindcasts performed with the spectral wave prediction model CREST. The spectral energy balance equation, including bottom friction and wave–bottom scattering source terms, was integrated numerically for selected time periods with swell-dominated conditions. Incident wave spectra at the model boundary were estimated from buoy measurements near the shelf break, assuming weak spatial variations in the offshore wave field. The observed strong and variable decay of the significant wave height across the shelf is predicted accurately with an overall scatter index of 0.15. Predicted wave directional properties at the peak frequency also agree well with observations, with a 5° root-mean-square error on the mean direction at the peak frequency and a 0.22 scatter index for the directional spread. Slight modifications are proposed for the laboratory-based empirical constants in the movable bed bottom friction source term, reducing the wave height scatter index to 0.13. A significant negative bias in the predicted directional spread (about –20%) suggests that other wave scattering processes not included in the energy balance equation broaden the wave field near the shore. Other residual errors may be largely the result of neglected spatial variations in the offshore wave conditions and, to a lesser extent, insufficient knowledge of the sediment properties.

1. Introduction

The formulation of the wave evolution problem in the form of an energy balance equation (Gelci et al. 1957) has been adopted widely in numerical wave prediction models because it effectively decouples the well understood linear propagation physics from the less clear forcing, scattering, and dissipation processes that are parameterized in the form of spectral “source terms” $S_i(\mathbf{k})$ on the right-hand side of the equation

$$\frac{dE(\mathbf{k})}{dt} = \sum_i S_i(\mathbf{k}). \quad (1)$$

The net rate of growth (or decay) of a spectral component, following the wave ray at its group velocity, is the sum of all source terms, each representing a clearly defined physical process. This equation is justified by the fact that substantial energy changes take place over time scales that are large compared with the wave period, with the notable exception of dissipation due to

wave breaking (Komen et al. 1994). It is also generally assumed that each process represented by a source term is locally independent of the other processes so that the same source term parameterization can be used in all circumstances as a function of the local wave spectrum and forcing conditions. The aim of the present paper is to provide a validation of the energy balance equation (1) for the relatively simple case of weak wind forcing, when the wave field is dominated by swell, affected primarily by wave–bottom interactions.

A direct validation of theories and parameterizations of source terms with observations is very difficult because their subtle effects on local wave properties (e.g., Reynolds stresses and nonlinear phase coupling of wave components) are often not detectable within the statistical uncertainty of the basic linear wave motion. Instead, source term parameterizations are usually verified by analyzing the cumulative changes in the wave field over a distance or time much larger than the wave period or wavelength, for example, the widely used fetch-limited growth curves for the wind wave generation problem. Although the effects of source terms are readily observed over hundreds of wavelength, the evolution is often the result of several processes, thus complicating

Corresponding author address: Dr. Fabrice Ardhuin, EPSHOM/CMO, 13 rue du Chatellier, Brest, Cedex 29609, France.
E-mail: ardhuin@shom.fr

the validation of individual source terms. Reviews of attempts to separate the effects of bottom friction, percolation, elasticity and scattering in observations of swell are given by Weber (1994) and Cavaleri (1994a,b).

Extensive observations in the Joint North Sea Wave Project (JONSWAP: Hasselmann et al. 1973) revealed that swell was attenuated in shallow water by bottom friction and that the relative reduction in the wave height is marginally more pronounced for increasing near-bottom velocities (Hasselmann et al. 1973, p. 89). This observation signaled a failure of the quadratic drag formulation with constant drag coefficient proposed previously by Hasselmann and Collins (1968) and led to a linear bottom friction source term (Bouws and Komen 1983) in the form

$$S_{\text{fric},J}(\mathbf{k}) = -\Gamma E(\mathbf{k}) \frac{(2\pi f)^2}{g^2 \sinh^2(kH)}, \quad (2)$$

where Γ is an empirical constant. This ‘‘JONSWAP’’ bottom friction source term provided reasonable estimates of the JONSWAP swell decay observations, although there was an order of magnitude scatter in the inferred values of Γ . Hasselmann et al. (1973) justified the form of (2) with the assumption that the wave orbital velocities were weak compared with the mean (tidal) currents, but the predicted tidal modulation of the coefficient Γ was not observed. Following the early recognition by Zhukovets (1963) of the importance of wave-generated bedforms and theoretical work on turbulent oscillatory boundary layers (e.g., Kajiura 1968; Grant and Madsen 1979), Grant and Madsen (1982) combined bottom roughness and boundary layer parameterizations in the first model capable of predicting bottom friction over a movable bed. Potential effects of such a parameterization were investigated by Graber and Madsen (1988) and Tolman (1994, see his discussion for practical wave decay scales), and first verified recently using field data (Ardhuin et al. 2001; 2003, hereinafter Part I). However the simple bottom friction source term (2) with $\Gamma = 0.038 \text{ m}^2 \text{ s}^{-3}$ is still widely used in scientific, engineering and operational wave modeling, although there is no justification (except for weak empirical evidence) for the form of (2) or the value of Γ . The relative success of (2) with a constant value of Γ may be explained by the fact that it describes qualitatively the decrease in bottom drag with increasing forcing expected on a movable bed. Expressing (2) in the general form of a movable bed parameterization [Part I, Eq. (5)] it follows that the equivalent dissipation coefficient $f_e = 2\Gamma/(gu_b)$ decreases with increasing bottom velocity u_b , capturing the variations in bottom roughness from low energy conditions, with relic bedforms, to high energy conditions when seabed ripples are obliterated by strong orbital flows. However, the constant Γ does not describe the sharp increase in bottom roughness in the intermediate range of conditions where active generation of ripples is expected (Fig. 1).

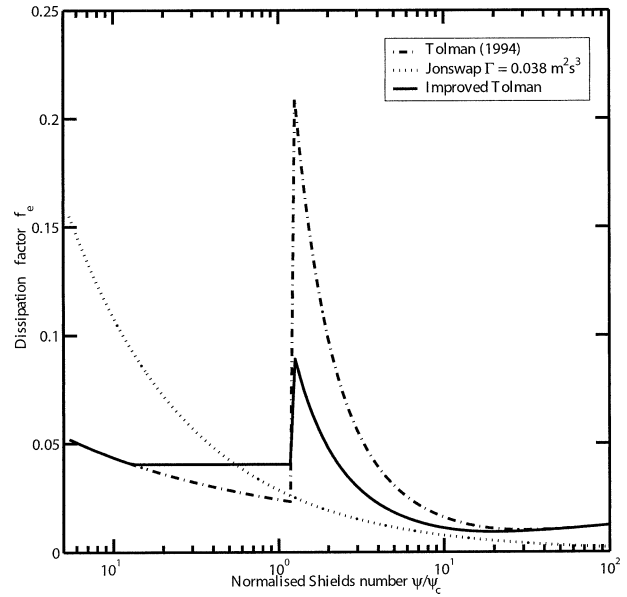


FIG. 1. Dissipation factors f_e as a function of the Shields number ψ normalized by its critical value ψ_c for sediment motion. The original parameterization proposed by Tolman (1994) based on the Madsen et al. (1990) laboratory experiments is compared with a slightly modified formulation tuned to the field data (see Part I) and the widely used JONSWAP parameterization.

Thus this simple linear formulation generally works better than quadratic friction models with a constant drag coefficient (e.g., Hasselmann and Collins 1968), although it severely underestimates the dissipation in active ripple conditions (Ardhuin et al. 2001). Assuming a constant bottom roughness rather than a constant Γ can improve wave predictions for a limited range of conditions (e.g., Johnson and Kofoed-Hansen 2000), but in practice the seabed roughness is unknown and variable and must be parameterized. In the present paper we test a movable bed bottom friction model that determines the bottom roughness from known sediment properties and wave forcing. The model validation uses data from the North Carolina continental shelf, which is essentially covered by fine and medium sand (Part I, Fig. 6).

Among other possible swell dissipation mechanisms, percolation was estimated to be much smaller than bottom friction for fine to medium sand and significant only for coarser sediments, while bottom elasticity is only important over sediments composed of mud or decomposed organic matter (Shemdin et al. 1980). Both processes will be neglected here. In addition to dissipative processes, backscattering of waves by the bottom topography may cause attenuation of waves toward the shore (Long 1973), but the estimated wave decay over actual bathymetry at the JONSWAP site and on the North Carolina shelf is extremely weak (Richter et al. 1976; Ardhuin and Herbers 2002). However, forward scattering of waves can cause significant broadening of wave directional spectra (Ardhuin and Herbers 2002;

TABLE 1. Wave-measuring instruments deployed during DUCK94 and used in the present study.

Name	Type	Water depth (m)	Directional	Operated by
8M	Pressure array	8.0	Yes	FRF
WR (FRF)	Buoy	17.0	No	FRF
44104	Buoy	49	Yes	NDBC
CHLV2	Laser gauge	15	No	NDBC
DSLN7	Laser gauge	18	No	NDBC
A	Pressure gauge	12	No	NPS
B	"	21	No	NPS
C	"	26	No	NPS
D	"	34	No	NPS
E	"	35	No	NPS
F	"	33	No	NPS
G	"	46	No	NPS
H	"	49	No	NPS
I	"	87	No	NPS

Part I), and the importance of this process is investigated below.

In the present paper, model hindcasts of the energy balance (1), restricting source terms to bottom friction and scattering, are compared with measurements from two field experiments, DUCK94 and SHOWEX, that took place in the same region of the North Carolina continental shelf. Datasets used in this study are briefly described in section 2, followed by a description of the model setup and source term formulations in section 3. Statistical comparisons of model results and observations are discussed in section 4. Conclusions and recommendations for swell forecasting in shallow water are given in section 5.

2. Datasets

The 1999 SHOWEX experiment, described in Part I, and the earlier DUCK94 experiment (Herbers et al. 2000) both took place on the continental shelf offshore of the North Carolina Outer Banks. In 1994 a transect of nine bottom-mounted pressure sensors, named A–I, was deployed from August to December (see Part I, Fig. 2 for instrument locations). Additional observations were available from the National Data Buoy Center (NDBC) 3-m discus buoy 44014, and a pressure sensor array and Waverider buoy maintained by the U.S. Army Engineer Field Research Facility (FRF), see Table 1 for a list of instruments in operation during DUCK94.

To exclude data records with significant local atmospheric forcing and wave breaking, the present analysis was restricted to swell-dominated conditions defined by the following conservative criteria:

- a peak frequency f_p less than 0.12 Hz for SHOWEX and 0.1 Hz for DUCK94 and
- a maximum sustained wind speed less than 60% of the linear wave phase speed at the peak frequency $C(f_p)$.

A lower f_p limit was used for DUCK94 because of the strong attenuation of wave signals in the bottom pressure measurements at the outer shelf sites. The latter criterion was chosen to exclude low-frequency wind waves generated on the shelf in extreme wind conditions, such as during the Hurricane Floyd landfall in 1999. The estimates of $C(f_p)$ are based on data from buoy WR(FRF), on the inner shelf. Waves propagate faster in deeper water, and thus these estimates for 15-m depth are a lower bound for wave speeds on the shelf. The wind speed here is taken to be the maximum of 1-h averaged values $U_{19.5}$ measured at 19.5 m above sea level at the end of the FRF pier (close to the 8M array) and U_5 measured at 5 m above sea level on board NDBC buoy 44014. Differences between wind speeds measured at the FRF pier and 44014 are generally small, except for an apparent time lag associated with the motion of weather systems. The two estimates are expected to roughly bracket wind forcing conditions over the entire shelf. The criteria for the selection of swell-dominated conditions were applied not only to the selected data record but also during the preceding 3 h, a period that corresponds to the propagation time of 0.08 Hz waves across the shelf. The selected swell-dominated time periods (indicated in black in Figs. 2b and 3b) are generally associated with distant storms or the early arrival of low-frequency waves from approaching storms (Figs. 2a and 3a). In contrast to SHOWEX, the DUCK94 data contain few energetic swell events, but include calm days with long-period, low-amplitude ($H_s < 0.5$ m) swell from distant sources (e.g., 10–12 and 15–18 September in Fig. 3).

3. Source terms

The implementation of the spectral wave prediction model CREST is described in Part I. Hindcasts were performed for the entire dataset using different combinations of source terms to evaluate their impact on the model skill. These model runs are summarized in Table 2.

A run without source terms (run 1) was included to isolate the effects of refraction and shoaling in the observed transformation of swell across the shelf. To identify the effects of individual source terms, hindcasts are presented with bottom friction only (run 2) and with Bragg scattering only (run 3). Runs 4a–c include both source terms with various parameterizations of bottom friction. The default bottom friction source term $S_{\text{fric,M}}$ used in model runs 2, 4c, 5, and 6 is a modification of Tolman's (1994) source term $S_{\text{fric,T}}$ (used in run 4b). Whereas $S_{\text{fric,T}}$ uses coefficients $A_1 = 1.5$, $A_2 = -2.5$, $A_3 = 1.2$, and $A_4 = 0$ [see Part I, Eqs. (6)–(12) that are based on earlier laboratory experiments], the modified form $S_{\text{fric,M}}$ uses coefficients $A_1 = 0.4$, $A_2 = -2.5$, $A_3 = 1.2$, and $A_4 = 0.05$, which were tuned to give a better overall agreement with DUCK94 and SHOWEX field observations. For reference and comparison with earlier

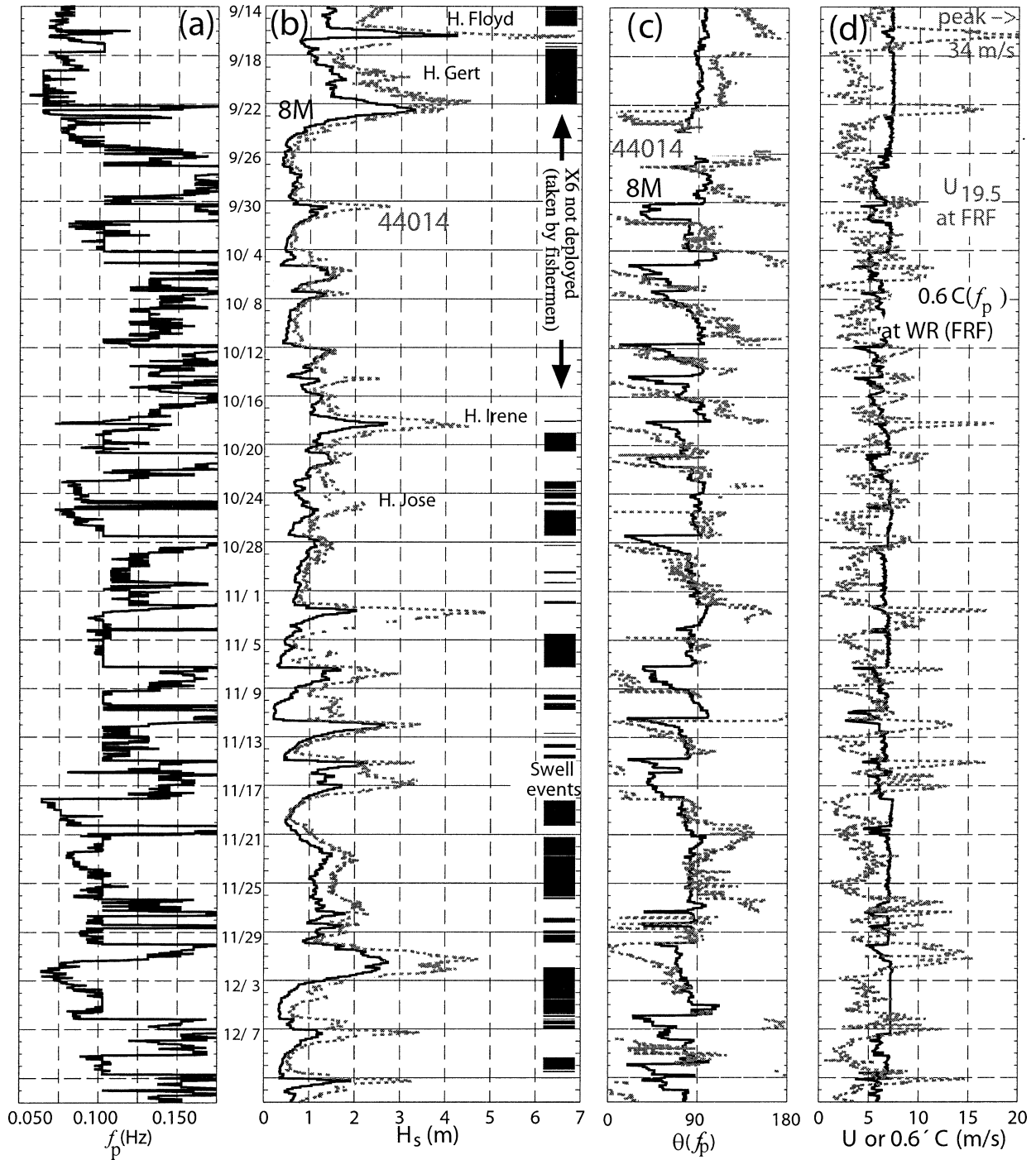


FIG. 2. Wave and wind conditions during SHOWEX: (a) Peak frequency f_p at buoy 44014. (b) Significant wave height and (c) mean direction at the peak frequency f_p for buoy 44014 and the 8M array. Dark bands in (c) indicate swell-dominated conditions, defined here as periods when (d) the wind speed is less than 60% of the wave phase speed at the peak frequency on the inner shelf.

work, run 4a uses the JONSWAP bottom friction source term $S_{\text{fric},J}$. Figure 1 compares the equivalent dissipation factors f_e of the different source term parameterizations.

The wave-bottom Bragg scattering source term S_{Bragg} is given in Part I Eq. (3) with an average bottom elevation spectrum estimate F_1^B (Fig. 6 in Part I) applied

to the entire shelf. The sensitivity of hindcasts to errors in the bottom spectrum estimate are assessed in run 5a, using the same settings as run 4c but with a different spectrum F_2^B , also uniform in space. In F_2^B the spectral levels for small-scale features (wavelengths less than 500 m) are taken from multibeam sonar surveys per-

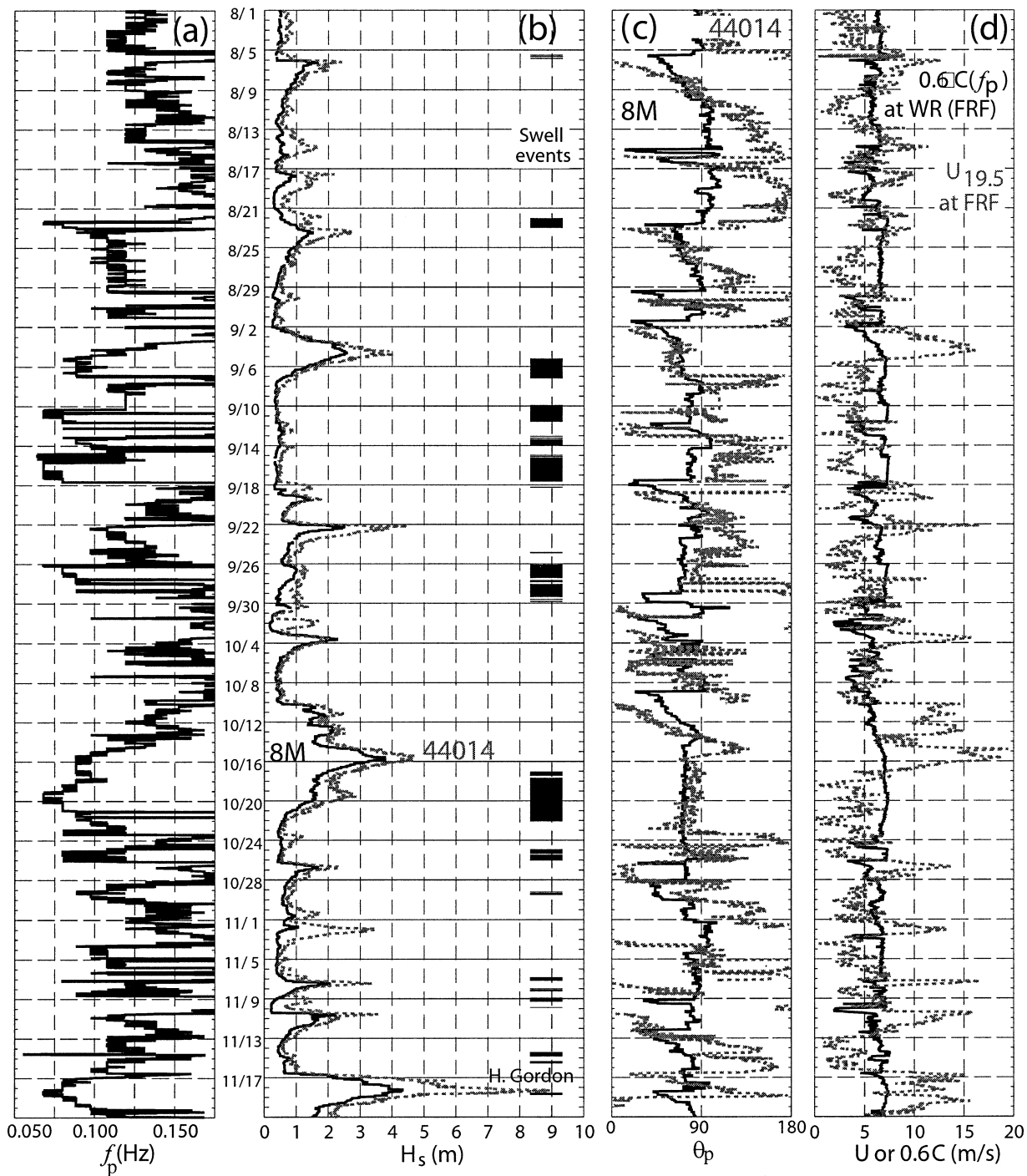


FIG. 3. Same format as Fig. 2 but for DUCK94.

formed during SHOWEX at a 25-m-depth site, rather than the 20-m-depth site used for F_1^B . Since the bottom elevation variance is less for F_2^B than for F_1^B , the effect of Bragg scattering is reduced [see Ardhuin and Herbers (2002) for other similar tests].

In the DUCK94 hindcasts, wave spectra at the offshore boundary are determined entirely from measure-

ments at buoy 44014, close to the shelf break, rather than the interpolation of two offshore buoys X6 and 44014 used for SHOWEX. The model was also run for SHOWEX using X6 data only (run 6) to evaluate errors due to the treatment of the offshore boundary. Tests of different frequency (10% instead of 5% exponential frequency grid) and directional resolutions (3° , 5° , and

TABLE 2. Model settings for different runs. The “rough shelf” runs use bottom elevation spectrum F_1^B to evaluate S_{Bragg} , whereas F_2^B is used in the “smooth shelf” run 5.

Run	S_{fric}	S_{Bragg}	Data for offshore boundary condition
1	0	0	44014 and X6
2	Modified Tolman $S_{\text{fric,M}}$	0	44014 and X6
3	0	Rough shelf	44014 and X6
4a	JONSWAP $S_{\text{fric,J}}$	''	44014 and X6
4b	Tolman (1994) $S_{\text{fric,T}}$	''	44014 and X6
4c	Modified Tolman $S_{\text{fric,M}}$	''	44014 and X6
5	Modified Tolman $S_{\text{fric,M}}$	Smooth shelf	44014 and X6
6	Modified Tolman $S_{\text{fric,M}}$	Rough shelf	X6

10°) gave very similar results except for a slight (1°–2°) increases in directional spread for 10° resolution, indicating that the predictions presented here are insensitive to the spectral discretization (see also Ardhuin and Herbers 2003, manuscript submitted to *J. Atmos. Oceanic Technol.*).

4. Model–data comparisons

To objectively assess the accuracy of source term parameterizations in the energy balance equation (1), a statistical analysis of swell hindcast results for the North Carolina continental shelf is presented here. Based on the criteria for swell-dominated conditions described above, the 725 3-h DUCK94 records (91 days) were reduced to 121 records (15 days), and the 2100 1-h SHOWEX records (87 days) were reduced to 528 records (22 days). Fewer records were available for some instruments, in particular A, B, and WR(FRF) which failed during the 1994 Hurricane Gordon, and X6, which malfunctioned at the peak of the 1999 Hurricane Floyd. The period from 22 September to 15 October 1999, when X6 was not in operation after being dragged by a fishing boat, was excluded from the analysis. The data processing procedures are described in Part I.

We present model–data comparisons of the significant wave height H_s and the mean direction θ_p and directional spread $\sigma_{\theta,p}$, both at the peak frequency f_p (see Part I for definitions). The directional properties of the waves, influenced primarily by refraction and Bragg scattering as shown in Part I, are discussed first. Only SHOWEX data are used in these comparisons because the DUCK94 data included few directional measurements. This is followed by an analysis of the wave heights, influenced by bottom friction and refraction, using both DUCK94 and SHOWEX hindcasts. For all three parameters the model errors generally grow across the shelf towards the shore but significant errors are already noted at the instruments located close to the offshore boundary. These model initialization errors are discussed last.

a. Mean wave direction

The mean wave direction at the peak frequency θ_p is predicted well by the model with no source terms or

bottom friction only, with a slight negative bias that increases across the shelf to a maximum value of 6° at 8M. The corresponding root-mean-square (rms) error is fairly uniform across the shelf (about 8°) with the exception of larger fluctuations (about 15°) at X5. These errors are small as compared with the strong refraction of wave directions across the shelf. For example, swell from Hurricane Floyd with offshore directions of 160° are refracted to 90° at 8M. The relatively large bias at 8M is not observed in hindcasts of DUCK94 swells (–1.6° bias, and rms error 6.9°) and may be related to a change in bottom topography not represented in the bathymetry grid used for ray computations. Errors at X5 are anomalously large. As discussed in Part I, large oscillations of θ_p (90°–140°) were observed at X5 when the offshore direction at X6 was varying over a narrow 110°–130° range. These results suggest that the wave rays are bent by refraction over bottom features not resolved in the sparse bathymetric surveys conducted on the outer shelf (Herbers et al. 2000).

Curiously, the addition of Bragg scattering in the model biases the mean direction farther to the north and increases the rms error by about 6°. This enhanced bias is likely due to the anisotropy of the bottom elevation spectrum used in the hindcasts (at wavelengths less than 500 m) based on a survey of only a small portion of the shelf [see Ardhuin and Herbers (2002) for further discussion]. The apparent increases in model bias and rms error are partially eliminated in hindcasts with both Bragg scattering and bottom friction (cf. runs 3 and 4 in Fig. 4) because spurious, obliquely scattered waves in the model propagate greater distances over the shelf, and thus are more strongly damped by bottom friction than the dominant waves that travel at near-normal angles to the depth contours.

Although some uncertainty remains in the local effects of topographic features on θ_p , the overall effect of refraction across the shelf, reducing the range of wave directions from 40°–160° at 44014 near the shelf break to 60°–100° near the shore at 8M (Fig. 4; Part I, Fig. 10c) is reproduced well by the model hindcasts.

b. Directional spread

The observed directional spread at the peak frequency $\sigma_{\theta,p}$ is relatively uniform across the shelf, generally decreasing slightly toward the coast. Observations at X6 range from 10° to 55° with typical values between 30° and 40°, whereas observations at 8M vary between 12° and 27° with typical values of 15°–25° (Fig. 4). However, when the offshore directional spectrum is very narrow ($\sigma_{\theta,p} < 20^\circ$), $\sigma_{\theta,p}$ increases toward the shore (Fig. 5; see also Part I), especially over the inner shelf between X3 and 8M.

Statistics from model runs with different source terms (Fig. 6) clarify how bottom friction and wave–bottom Bragg scattering contribute to $\sigma_{\theta,p}$. Run 1, without source terms, containing only the narrowing effect of

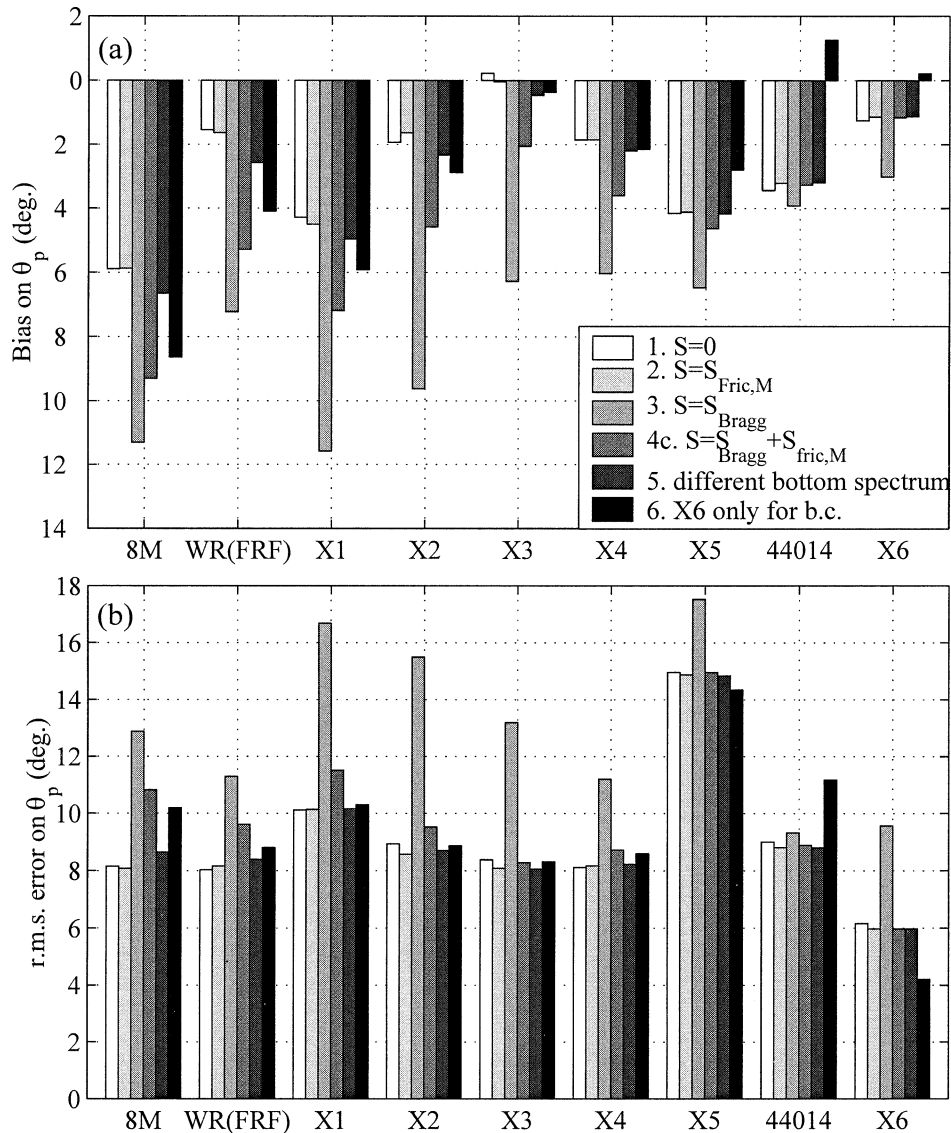


FIG. 4. Error statistics for predictions of the mean direction at the peak frequency θ_p : (a) Model bias and (b) rms error for swell-dominated periods observed during SHOWEX. Runs 1–4 use different combinations of source terms (Table 2). Run 5 uses a bottom elevation spectrum with a lower variance at small scales to evaluate the Bragg scattering source term. Run 6 is forced at the offshore boundary with X6 data only instead of the interpolation of X6 and 44014 data used in all other runs. Positive values in (a) correspond to a clockwise bias.

refraction as waves approach the shore, grossly underestimates $\sigma_{\theta,p}$ on the inner shelf with a typical bias of -10° . In run 2, the addition of bottom friction narrows the spectrum even further because waves propagating at larger angles relative to the depth contours have a longer propagation time across the shelf, and thus are more exposed to dissipation. Wave–bottom Bragg scattering opposes these two narrowing effects by diffusing the energy around the mean direction (Ardhuin and Herbers 2002). While Bragg scattering alone tends to give spectra that are too broad on the middle of the shelf (Fig. 6, run 3), the hindcast that includes the combined

effects of Bragg scattering and bottom friction generally yields good agreement (Fig. 6), reducing the scatter index at site 8M on the inner shelf from 0.51 (run 2) to 0.25 (run 4).

Predicted Bragg scattering effects are most pronounced for narrow offshore spectra, approximately doubling the directional spread at 8M (cf. diamonds and triangles in Fig. 5), in good agreement with the observations (crosses). For broad offshore spectra ($20 < \sigma_{\theta,p} < 40^\circ$ at X6) predicted scattering effects are weaker, yielding spectra at 8M that are about 5° – 10° narrower than the observed spectra. The predicted scattering ef-

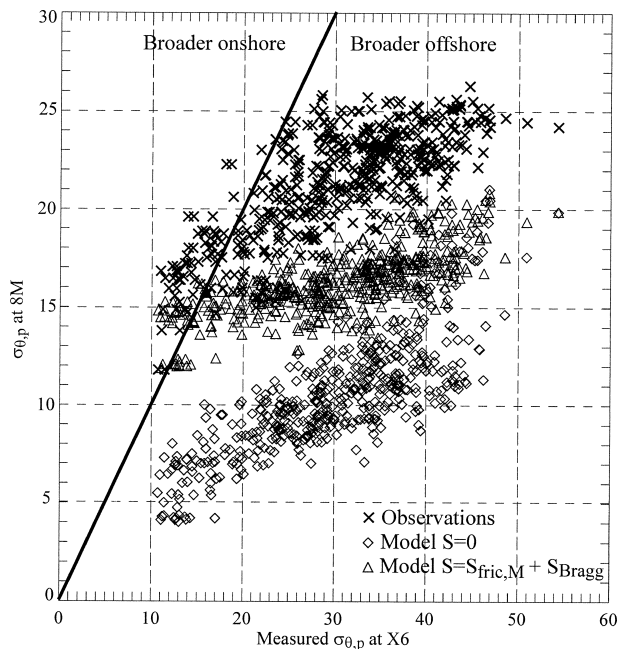


FIG. 5. Observed and modeled directional spread at the peak frequency $\sigma_{\theta,p}$ observed near the shore at 8M vs $\sigma_{\theta,p}$ observed offshore at X6. The solid line separates spectra that are broader in the nearshore and spectra that are broader offshore.

fect is strongest for wave spectra with low peak frequencies (Fig. 7), but these low-frequency swells tend to have the narrowest offshore directional spectra so that the influence of the spectral width and peak frequency on wave-bottom scattering cannot be clearly separated in these results.

Model hindcasts are sensitive to the choice of the bottom elevation spectrum. The bottom spectrum used here (run 4) includes large-amplitude, small-scale topographic features not found everywhere on the shelf, and thus the predictions likely exaggerate the true effect of wave-bottom Bragg scattering across this continental shelf. Run 5 using a seabed spectrum with reduced small-scale variance, characteristic of smoother mid-shelf regions, accounts only partially for the observed increase in $\sigma_{\theta,p}$ (Fig. 6, run 5). The negative bias of $\sigma_{\theta,p}$ predictions suggests that other processes are important. Higher order wave-bottom Bragg scattering (Liu and Yue 1998) and nonlinear wave-wave scattering (Hasselmann 1962) may cause additional broadening not included in the present hindcast.

Errors also result from the unknown directional dependence of bottom friction damping rates. The bottom friction source term was assumed somewhat arbitrarily to be isotropic. A quadratic drag law would give a difference between the major and minor principal axes of the directional dissipation source term that is as large as a factor of 2 for unidirectional waves (Hasselmann and Collins 1968). This type of anisotropy would cause more dissipation for waves with directions along the mean direction and less dissipation in perpendicular di-

rections, therefore increasing the directional spread. The absence of wave reflection from the beach in the model is another possible source of a negative bias. Even though offshore traveling waves are removed from the high-resolution directional spectrum used to compute $\sigma_{\theta,p}$ at the 8M array site, they contribute to the $\sigma_{\theta,p}$ estimates obtained from buoys farther out on the shelf. However, earlier studies at the same site (Elgar et al. 1994) show that reflection from the beach is significant only with extremely low energy swell conditions ($H_s < 0.3$ m), not observed during SHOWEX.

c. Wave height

For the analysis of wave height predictions the SHOWEX dataset is augmented with the DUCK94 data. Statistics given below combine results at DUCK94 and SHOWEX instruments located in the same area (such as pressure gauge C and buoy X2) or water depths (such as pressure gauge G and buoy X5). Changes in the peak frequency across the shelf are negligible, but the significant wave height H_s generally decreases from offshore to nearshore. For moderate energetic swell the observed H_s at 8M are about one-half of the observed values at X6, while a smaller reduction (~25%) is observed in benign conditions ($H_s < 1.5$ m at X6). This effect is explained only in part by refraction that reduces the wave heights of waves that propagate onshore at large oblique angles relative to the depth contours. Indeed, the model without source terms (Fig. 8, run 1), which accounts only for the effects of refraction and shoaling, overpredicts wave heights with a typical bias of 0.2 m on the inner shelf and gives an overall (average for all sensors) scatter index of 0.26 for H_s . Adding Bragg scattering increases the positive H_s bias because the longer residence time of waves on the shelf increases the wave energy in the absence of dissipation, degrading the overall scatter index to 0.29 (Fig. 8, run 3).

Including bottom friction reduces the model errors dramatically. Run 4b, using Tolman's (1994) movable-bed source term based on laboratory data without any empirical tuning to field conditions, reduces the overall scatter index of H_s predictions from 0.29 to 0.15 (Fig. 8). This result supports the hypothesis that the observed formation of vortex ripples by energetic swell (Ardhuin et al. 2002), and their feedback on the waves through enhanced bottom roughness is a primary mechanism for wave attenuation across a sandy continental shelf. However, a negative bias of -9 cm at 8M indicates a model tendency to overestimate dissipation, already noted by Ardhuin et al. (2001). The slightly modified Tolman source term $S_{fric,M}$ (with coefficients tuned to the observations) gives an overall scatter index of 0.13 with a maximum of 0.20 at X2 (run 4c in Fig. 8).

On average the empirical JONSWAP bottom friction source term performs about equally well (Fig. 8, run 4a), giving an overall scatter index of 0.16. However, this source term gives poor results at CHLV2, a site

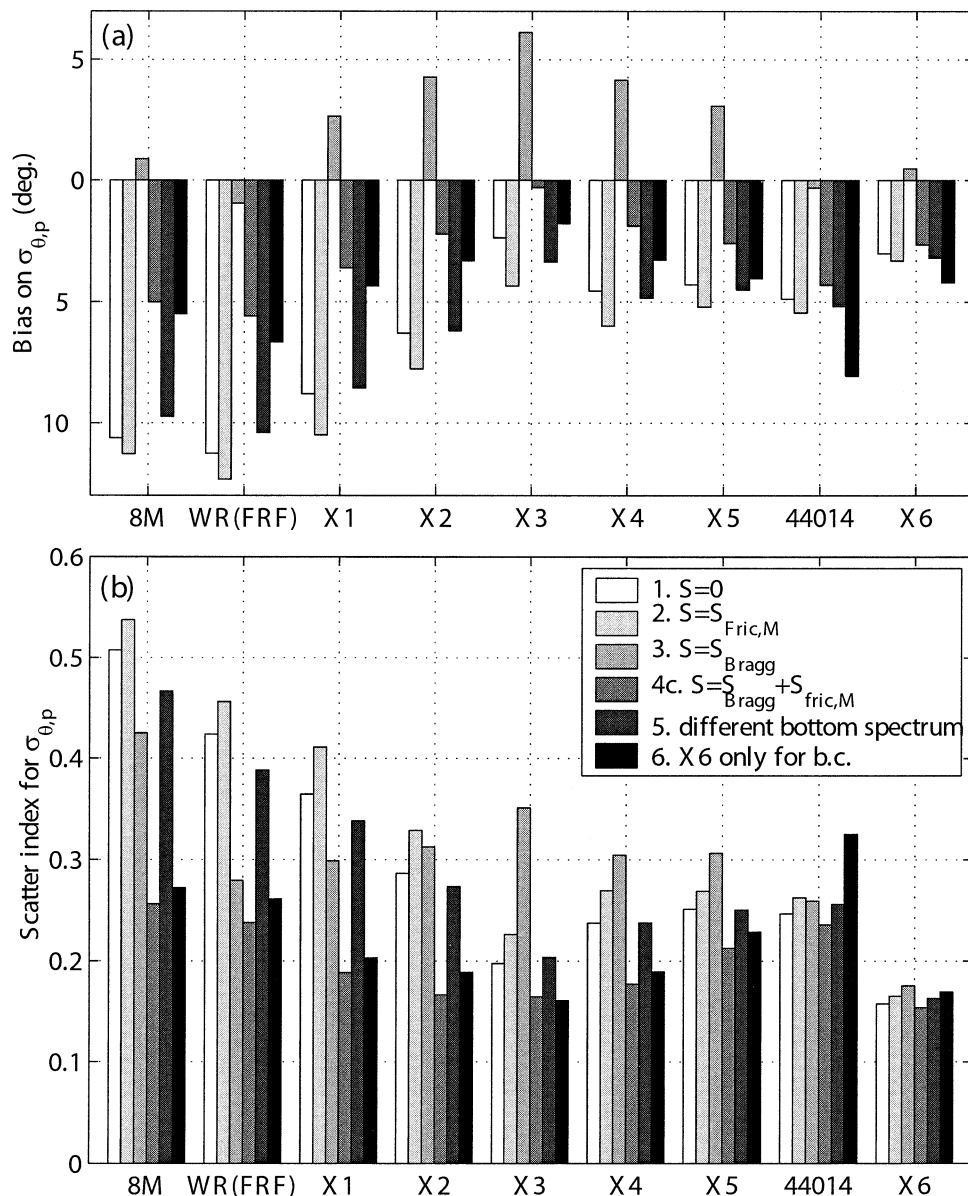


FIG. 6. Error statistics for predictions of the directional spread at the peak frequency $\sigma_{\theta,p}$. Same format as in Fig. 3. The scatter index is defined as the ratio of the rms error and the observed rms value.

located inshore of shallow shoals (20-m depth; see Part I Fig. 2), with a scatter index of 0.53 and a positive bias of 20 cm. This bias is the result of large model–data discrepancies during the arrival of swell from Hurricane Gert (17–21 September 1999). The observed strong dissipation, up to 93% of the incident wave energy flux, is likely the result of active ripple generation on the shoals offshore of CHLV2 (see Part I Fig. 12b), for which the JONSWAP source term grossly underpredicts the dissipation factor f_e (Fig. 1).

The dependence of model error statistics on the Shields number, estimated from wave measurements at representative inner shelf sites X3 (SHOWEX) and C (DUCK94), is shown in Fig. 9. The largest errors of a

nondissipative model (run 1) clearly occur for large values of the Shields number when the presence of active ripples is expected. The JONSWAP friction source term also gives the largest errors in this regime.

In contrast, the Tolman source term $S_{\text{fric,T}}$ significantly underestimates wave heights in active ripple conditions (Figs. 9g–i), suggesting that the ripples (observed on most of the shelf; see Arduin et al. 2002) were less rough than those in the Madsen et al. (1990) laboratory experiments. Ripples in the field may be significantly smoother than in the laboratory owing to the directional spreading of natural waves, as well as their formation on an initial bed configuration with relic bedforms. The present dataset is too limited to address effects of past

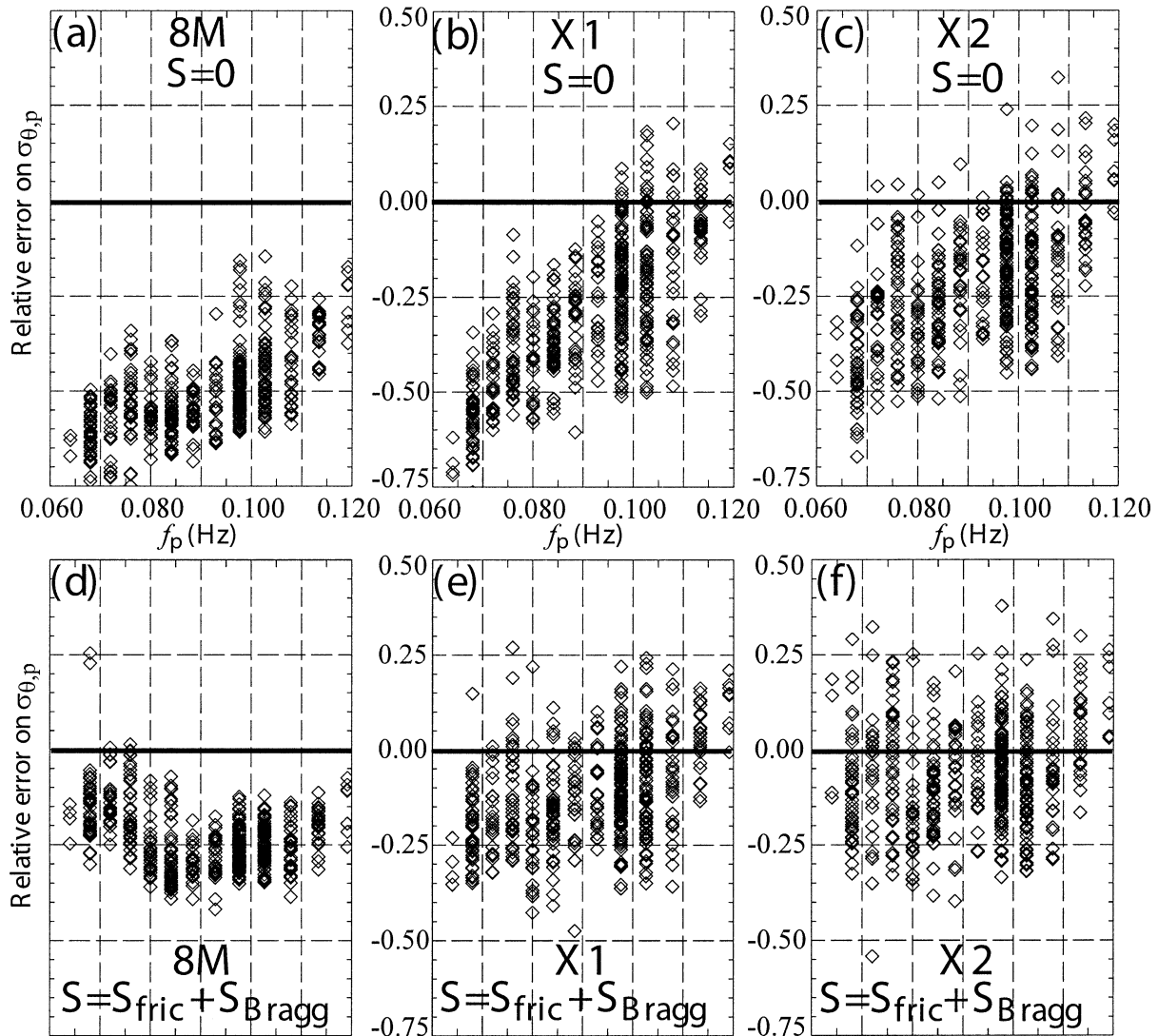


FIG. 7. Relative bias (normalized by the observed mean value) of the directional spread $\sigma_{\theta,p}$ vs the peak frequency f_p at inner shelf sites (a), (d) 8M, (b), (e) X1, and (c), (f) X2. (top) No source terms (run 1). (bottom) Bragg scattering and bottom friction (run 4c).

history of the bedforms or the possibly different adjustment of the ripple roughness in increasing, stable, or decreasing forcing conditions.

We have thus adjusted the A_1 – A_4 empirical coefficients to get a better overall agreement (run 4c, using $S_{\text{fric},M}$; Figs. 9j–l). The relic roughness coefficient A_4 is only important in the intermediate Shields number range where no active ripples are expected and can be rather well chosen. All three other coefficients play a role in the active ripple regime. Keeping the ripple threshold $A_3 = 1.2$ from Madsen et al. (1990) and the roughness decay exponent $A_2 = -2.5$, the model results are only weakly sensitive to the ripple roughness parameter A_1 . Indeed a parameterization with a large roughness will lead to a faster local wave decay, resulting in a reduction in wave height and decay rate closer inshore. This is a negative feedback loop. Thus model results are quali-

tatively similar when A_1 is reduced by a factor 4, from 1.5 to 0.4, which is done in run 4c. The parameterization $S_{\text{fric},M}$ used in that run brings the model in slightly closer agreement with the DUCK94 and SHOWEX data. The present tuning of the empirical parameters in the active ripple regime should therefore be considered with caution, the model performing almost equally well with values of A_1 between 0.4 and 1.5.

d. Uncertainties in offshore boundary conditions

Two important sources of model errors are the evaluation of the offshore wave field from only two buoys, X6 and 44014, and the estimation of a directional spectrum from buoys. Model errors at X6, when the boundary condition is determined from X6 data only (run 6), are entirely the result of the difference between offshore

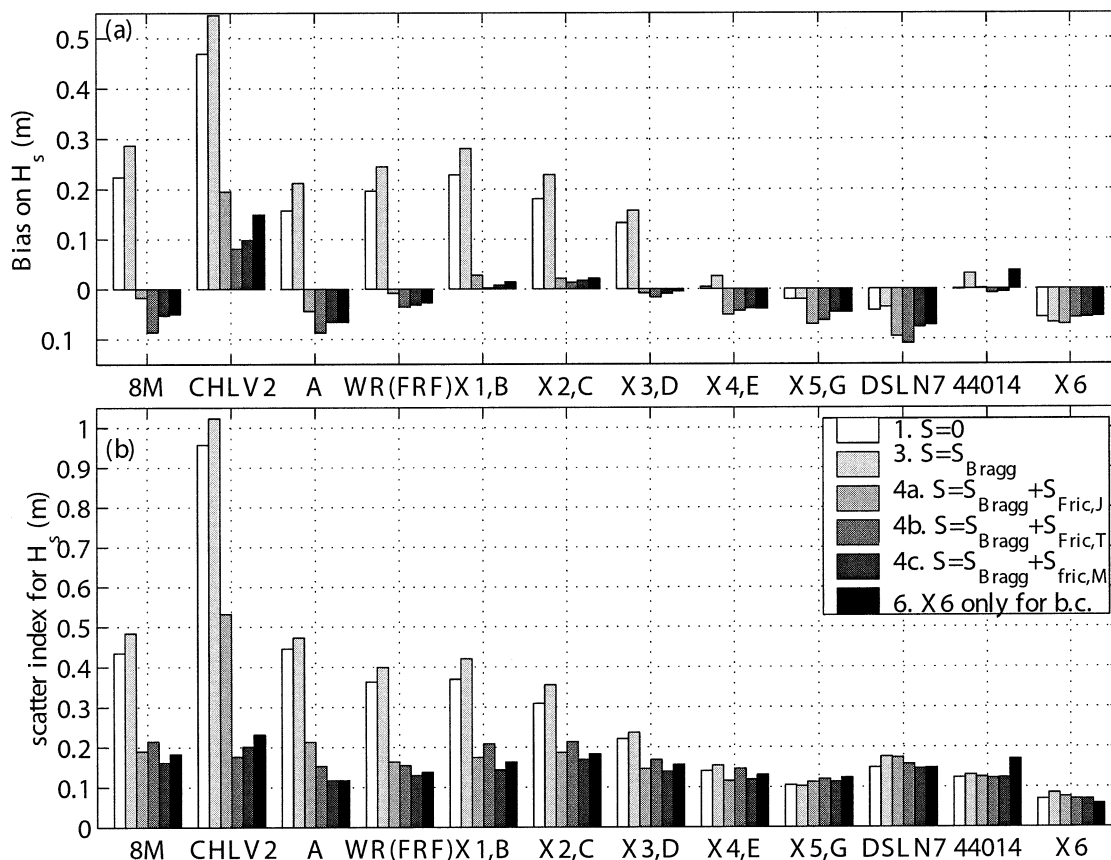


FIG. 8. (a) Model bias and (b) scatter index (ratio of rms error and rms value) for the significant wave height H_s in swell-dominated periods during SHOWEX and DUCK94.

propagating waves predicted by the model (as a result of refraction and backscattering) and those estimated from the buoy data. Whereas the scatter index for H_s is small (0.06), θ_p and $\sigma_{\theta,p}$ are more sensitive to weak offshore propagating components, giving an rms error of 5° for θ_p and a scatter index of 0.18 for $\sigma_{\theta,p}$.

Using only X6 for the model boundary condition enhances errors at 44014 (cf. runs 4c and 6 in Figs. 4, 6, and 8), possibly owing to propagation errors across the shelf break and spatial variations in the offshore wave field over the 60 km separating X6 and 44014. These offshore variations may be caused in part by wave-current refraction in the Gulf Stream and its eddies (Holthuijsen and Tolman 1991), often seen along the shelf break in sea surface temperature satellite images, and mesoscale fluctuations in the offshore wave field (Tournadre 1993). The $\sigma_{\theta,p}$ errors may further be influenced by differences in the response between a Waverider buoy (X6) and a 3-m discus pitch-and-roll buoy (44014), the latter giving generally larger directional spreads (O'Reilly et al. 1996).

The relatively large errors in predictions at sites near the shelf break indicate that measurement uncertainties and unknown variations in the wave field along the shelf break account for a significant fraction of the scatter

indices closer inshore, and thus further improvement of the model skill may require more comprehensive measurements of the incident wave field.

5. Discussion and conclusions

The evolution of swell across the North Carolina continental shelf was investigated with field data from the DUCK94 and SHOWEX experiments, covering a wide range of offshore wave conditions. The spectral wave prediction model CREST with a nondiffusive Lagrangian advection scheme and source terms for bottom friction and wave-bottom Bragg scattering was implemented on a large portion of the North Carolina-Virginia continental shelf, extending from deep water (1500-m depth) to the inner shelf (8-m depth). Observed significant wave heights, mean directions, and directional spreads are compared with model results obtained using various sets of source terms.

The predicted Bragg scattering effect of the small-scale (comparable with the surface wavelength) shelf topography explains most of the observed broadening of the wave spectrum toward the shore, which occasionally balances the narrowing caused by refraction over the quasi-plane large-scale bathymetry. Predicted

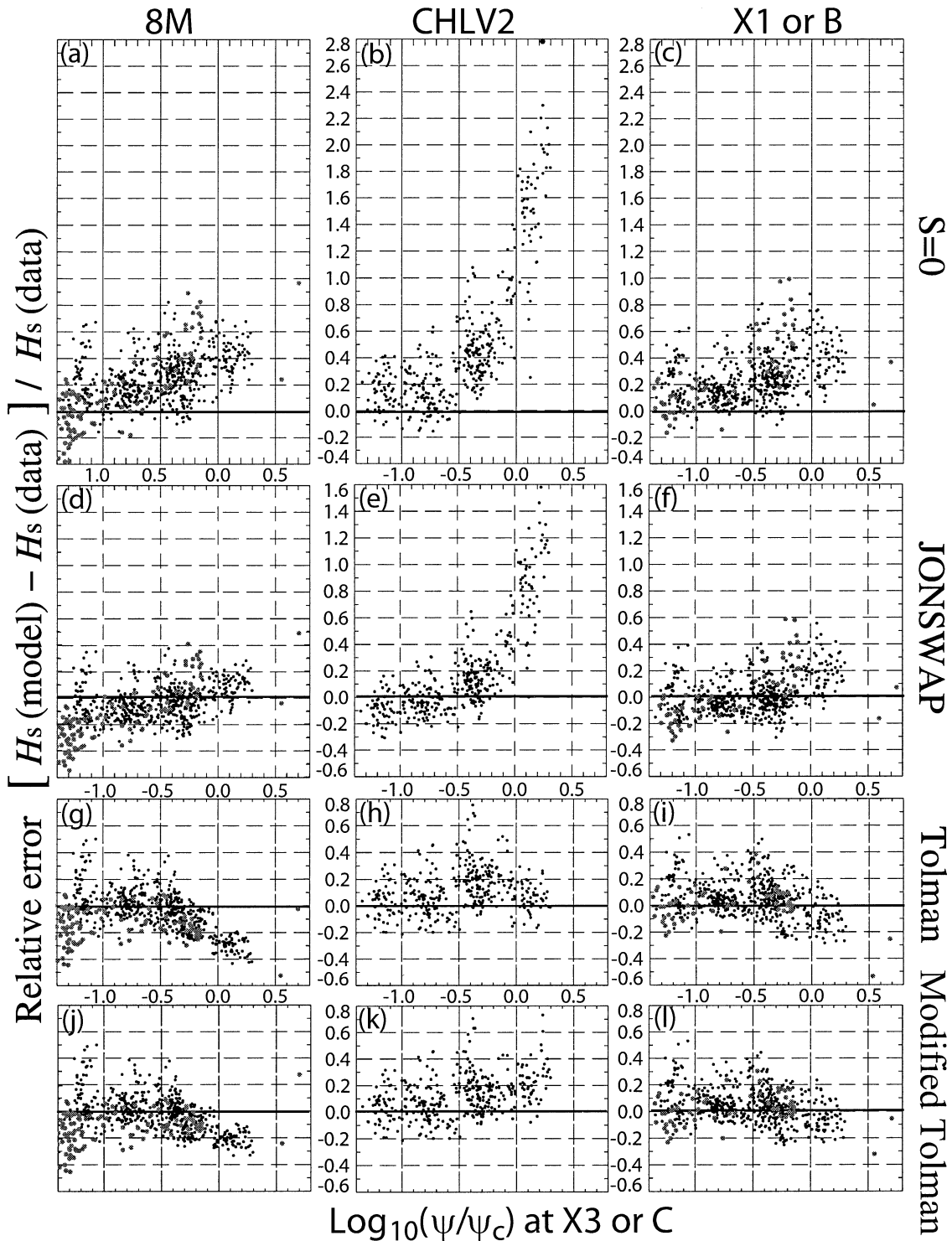


FIG. 9. Relative bias of H_s predictions vs Shields number (normalized by the critical value). Results are shown at three inner shelf sites, for different combinations of source terms, (a)–(c) $S = 0$, (d)–(f) $S = S_{\text{fric,J}} + S_{\text{Bragg}}$, (g)–(i) $S = S_{\text{fric,T}} + S_{\text{Bragg}}$, and (j)–(l) $S = S_{\text{fric,M}} + S_{\text{Bragg}}$. Larger gray dots correspond to 3-h DUCK94 records and smaller black dots correspond to 1-h SHOWEX records.

directional spectra are nevertheless still too narrow on the inner shelf (by about 20% as compared with 50% for hindcasts without Bragg scattering), possibly as a result of higher-order wave–bottom or wave–wave scattering, anisotropy in the bottom friction source term, and wave reflection from the beach, which are not represented in the present model. Errors may also result from the assumed spatially uniform spectrum of small-scale bottom topography, determined from a high-resolution survey of a small portion of the inner shelf.

Although the present results show that Bragg scattering plays an important role in the transformation of wave directional properties, the two-dimensional bottom elevation spectra needed to evaluate the source term are not always available. For practical applications a simpler form of the Bragg scattering source term may be desirable, for example, assuming a universal bottom elevation spectral shape. Although the physical diffusion effect of Bragg scattering appears essential for accurate modeling of narrow directional spectra, it may be partly masked by numerical diffusion and limited directional resolution of existing wave prediction models. Inadequate parameterizations of other source terms can artificially enhance directional spreads in the model results. Indeed, it is well known that the discrete interaction approximation (Hasselmann and Hasselmann 1985) yields a broader directional spectrum than the exact computation of the quartet wave–wave interactions. Applications to other regions with important small-scale topography (such as the sandwave areas in the North Sea) may help to assess the importance of incorporating wave–bottom Bragg scattering in operational wave prediction models.

The observed strong attenuation of energetic swell (inferred energy losses up to 93% of the incident wave energy flux) is reproduced well by Tolman's (1994) bottom friction source term, which accounts for the generation of sand ripples by waves and their feedback on the waves. This source term, based on careful laboratory studies by Madsen et al. (1990), without any further adjustment reduces the scatter index for predictions of the significant wave height H_s from 0.27, for energy conserving spectral refraction computations, to 0.15. An ad hoc increase of relic roughness and reduction of the ripple roughness by a factor 4 improves the hindcast results and reduces the overall scatter index for the wave heights to 0.13. The imperfect knowledge of the offshore boundary condition likely accounts for a significant fraction of the remaining errors.

Overall, the widely used empirical JONSWAP bottom friction source term has a skill (average scatter index: 0.16) comparable to Tolman's (1994) original movable bed source term, but occasionally yields much larger errors because it does not account for large increases in bottom roughness under active ripple conditions. The JONSWAP bottom friction parameterization is easy to use in practice because it requires no prior knowledge about bottom sediments, whereas the movable bed

source term requires some sediment information, and both are only valid for sandy bottoms. It should be emphasized that no parameterization has been tested in the sheet flow regime of very large Shields numbers $\psi/\psi_c > 5$ that occurs in severe storms.

To cover a wider range of bottom sediments, more general parameterizations of wave energy dissipation are needed that combine movable-bed effects, percolation for larger grain sizes, and a bottom elasticity model for cohesive sediments that can give even stronger wave damping (e.g., Forristall et al. 1990; Cavaleri 1994b).

In addition to the direct local effects of each source term, the numerical integrations of (1) reveal indirect effects of the combined source terms as waves propagate over a finite distance. In particular, Bragg scattering enhances the dissipation of wave energy owing to bottom friction by increasing the time of propagation of waves across the shelf. Overall the energy balance (1) with both movable bed bottom friction and wave–bottom Bragg scattering source terms, provides the best description of the observed swell evolution across the North Carolina continental shelf.

Acknowledgments. This research is supported by the Coastal Dynamics Program of the U. S. Office of Naval Research, the French Navy Hydrographic and Oceanographic Service, and the U.S. National Science Foundation (Grant OCE-0114875). Buoys X1 through X6 were deployed and maintained by staff from the Naval Postgraduate School and the Scripps Institution of Oceanography Center for Coastal Studies. We thank the crew of R/V *Cape Hatteras* for excellent support. Wave data from the 8-m-depth array and waverider buoy WR were provided by the Field Research Facility of the U.S. Army Engineer Waterways Experiment Station's Coastal Engineering Research Center, and data from buoy 44014 and C-MAN stations DSLN7 and CHLV2 were provided by the National Data Buoy Center (available online at <http://www.ndbc.noaa.gov>). Permission to use these data is appreciated. Both R. E. Jensen and C. Long generously helped us with the analysis of these data, and W. Birkemeier and the FRF staff provided flawless logistics support during SHOWEX. Bathymetric data was obtained from the U. S. National Oceanographic Data Center. F. Dobson, M. Donelan, and T. P. Stanton organized and collected the high-resolution multibeam bathymetry data on board the Canadian Garde Côtière vessel *F. G. Creed*. We note that M. Orzech contributed significantly to the synthesis of the bathymetry dataset. Fruitful comments and encouragement from T. P. Stanton, E. B. Thornton, R. E. Jensen, M. Donelan, and K. Belibassakis are gratefully acknowledged.

REFERENCES

- Ardhuin, F., and T. H. C. Herbers, 2002: Bragg scattering of random surface gravity waves by irregular sea bed topography. *J. Fluid Mech.*, **451**, 1–33.

- , —, and W. C. O'Reilly, 2001: A hybrid Eulerian–Lagrangian model for spectral wave evolution with application to bottom friction on the continental shelf. *J. Phys. Oceanogr.*, **31**, 1498–1516.
- , T. G. Drake, and T. H. C. Herbers, 2002: Observations of wave-generated vortex ripples on the North Carolina continental shelf. *J. Geophys. Res.*, **107**, 3143, doi:10.1029/2001JC000986.
- , W. C. O'Reilly, T. H. C. Herbers, and P. F. Jessen, 2003: Swell transformation across the continental shelf. Part I: Attenuation and directional broadening. *J. Phys. Oceanogr.*, **33**, 1921–1939.
- Bouws, E., and G. J. Komen, 1983: On the balance between growth and dissipation in an extreme depth-limited wind-sea in the southern North Sea. *J. Phys. Oceanogr.*, **13**, 1653–1658.
- Cavaleri, L., 1994a: Bottom elasticity. *Dynamics and Modeling of Ocean Waves*, G. J. Komen et al., Eds., Cambridge University Press, 341–343.
- , 1994b: Bottom scattering and bottom elasticity. *Dynamics and Modeling of Ocean Waves*, G. J. Komen et al., Eds., Cambridge University Press, 167–171.
- Elgar, S., T. H. C. Herbers, and R. T. Guza, 1994: Reflection of ocean surface gravity waves from a natural beach. *J. Phys. Oceanogr.*, **24**, 1503–1511.
- Forristall, G. Z., E. H. Doyle, W. Silva, and M. Yoshi, 1990: Verification of a soil wave interaction model (SWIM). *Modeling Marine Systems*, A. M. Davies, Ed., Vol. 2, CRC Press, 41–46.
- Gelci, R., H. Cazalé, and J. Vassal, 1957: Prévision de la houle. La méthode des densités spectroangulaires. *Bull. Inf. Comité Central Océanogr. Etude Côtes*, **9**, 416–435.
- Graber, H. C., and O. S. Madsen, 1988: A finite-depth wind-wave model. Part I: Model description. *J. Phys. Oceanogr.*, **18**, 1465–1483.
- Grant, W. D., and O. S. Madsen, 1979: Combined wave and current interaction with a rough bottom. *J. Geophys. Res.*, **84**, 1797–1808.
- , and —, 1982: Movable bed roughness in unsteady oscillatory flow. *J. Geophys. Res.*, **87** (C1), 469–481.
- Hasselmann, K., 1962: On the non-linear energy transfer in a gravity wave spectrum, Part I: General theory. *J. Fluid Mech.*, **12**, 481–501.
- , and J. I. Collins, 1968: Spectral dissipation of finite depth gravity waves due to turbulent bottom friction. *J. Mar. Res.*, **26**, 1–12.
- , and Coauthors, 1973: Measurements of wind-wave growth and swell decay during the Joint North Sea Wave Project. *Dtsch. Hydrogr. Z.*, **8** (12) (Suppl. A), 1–95.
- Hasselmann, S., and K. Hasselmann, 1985: Computation and parameterizations of the nonlinear energy transfer in a gravity-wave spectrum. Part I: A new method for efficient computations of the exact nonlinear transfer. *J. Phys. Oceanogr.*, **15**, 1369–1377.
- Herbers, T. H. C., E. J. Hendrickson, and W. C. O'Reilly, 2000: Propagation of swell across a wide continental shelf. *J. Geophys. Res.*, **105** (C8), 19 729–19 737.
- Holthuijsen, L. H., and H. L. Tolman, 1991: Effects of the Gulf Stream on ocean waves. *J. Geophys. Res.*, **96** (C7), 12 755–12 771.
- Johnson, H. K., and H. Kofoed-Hansen, 2000: Influence of bottom friction on sea surface roughness and its impact on shallow water wind wave modeling. *J. Phys. Oceanogr.*, **30**, 1743–1756.
- Kajiura, K., 1968: A model of the bottom boundary layer in water waves. *Bull. Earthquake Res. Inst. Univ. Tokyo*, **46**, 75–123.
- Komen, G. J., L. Cavaleri, M. Donelan, K. Hasselmann, S. Hasselmann, and P. A. E. M. Janssen, Eds., 1994: *Dynamics and Modelling of Ocean Waves*. Cambridge University Press, 532 pp.
- Liu, Y., and D. K. P. Yue, 1998: On generalized Bragg scattering of surface waves by bottom ripples. *J. Fluid Mech.*, **356**, 297–326.
- Long, R. B., 1973: Scattering of surface waves by an irregular bottom. *J. Geophys. Res.*, **78** (33), 7861–7870.
- Madsen, O. S., P. P. Mathisen, and M. M. Rosengaus, 1990: Movable bed friction factors for spectral waves. *Proc. 22d Int. Conf. on Coastal Engineering*, Delft, Netherlands, ASCE, 420–429.
- O'Reilly, W. C., T. H. C. Herbers, R. J. Seymour, and R. T. Guza, 1996: A comparison of directional buoy and fixed platform measurements of pacific swell. *J. Atmos. Oceanic Technol.*, **13**, 231–238.
- Richter, K., B. Schmalfeldt, and J. Siebert, 1976: Bottom irregularities in the North Sea. *Dtsch. Hydrogr. Z.*, **29** (1), 1–10.
- Shemdin, O. H., S. V. Hsiao, H. E. Carlson, K. Hasselmann, and K. Schulze, 1980: Mechanisms of wave transformation in finite depth water. *J. Geophys. Res.*, **85** (C9), 5012–5018.
- Tolman, H. L., 1994: Wind waves and moveable-bed bottom friction. *J. Phys. Oceanogr.*, **24**, 994–1009.
- Tournadre, J., 1993: Time and space scales of significant wave heights. *J. Geophys. Res.*, **98** (C3), 4727–4738.
- Weber, S. L., 1994: Bottom friction and percolation. *Dynamics and Modeling of Ocean Waves*, G. J. Komen et al., Eds., Cambridge University Press, 156–166.
- Zhukovets, A. M., 1963: The influence of bottom roughness on wave motion in a shallow body of water. *Izv. Akd. Nauk SSSR, Seriya Geofizicheskaya*, **10**, 1561–1570.